Gravitational Wave Measurements

Reed Essick
IPA Oct 9, 2018

Our detectors

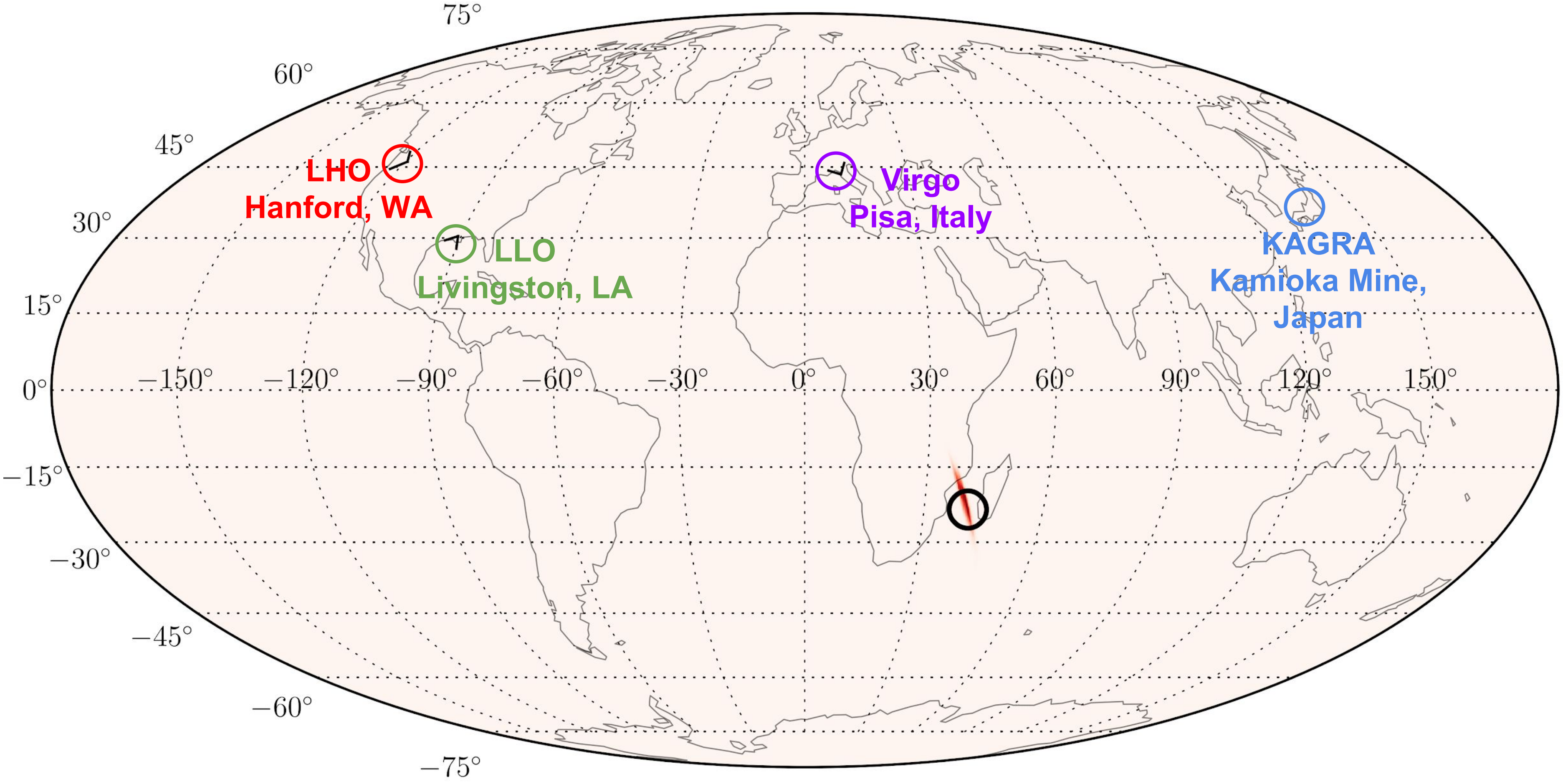

Our detectors

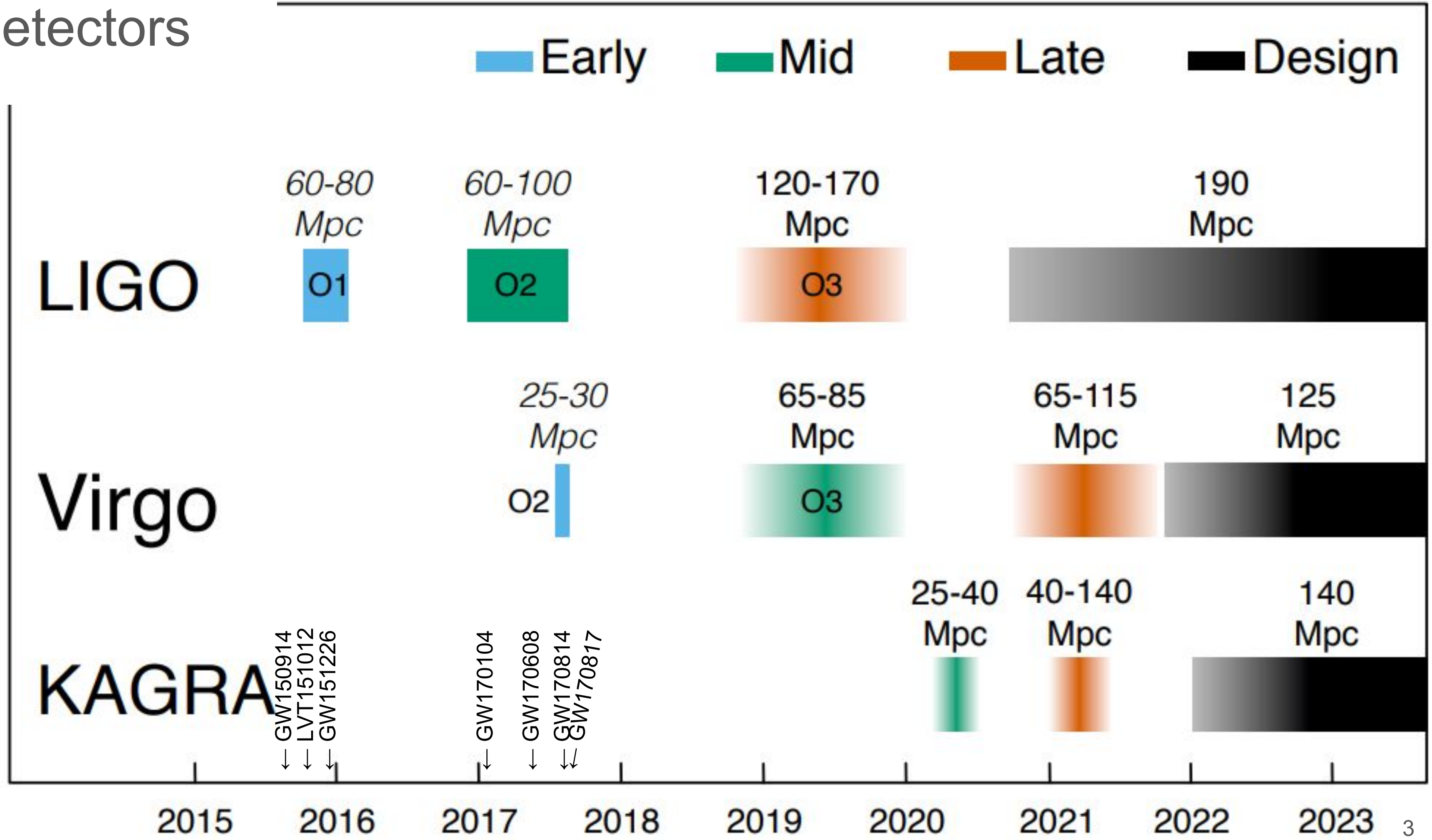

Abbott+(2018)

Our detectors

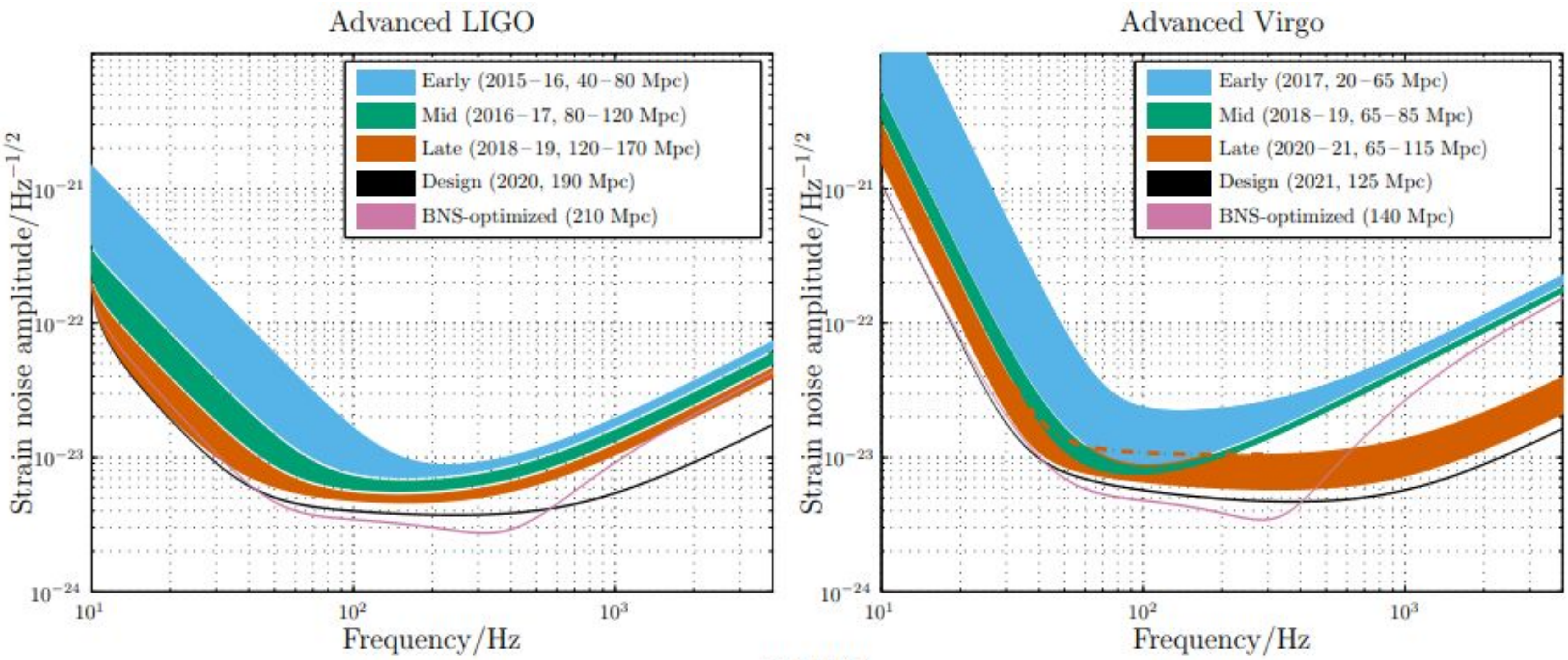

Abbott+(2018)

Our detectors

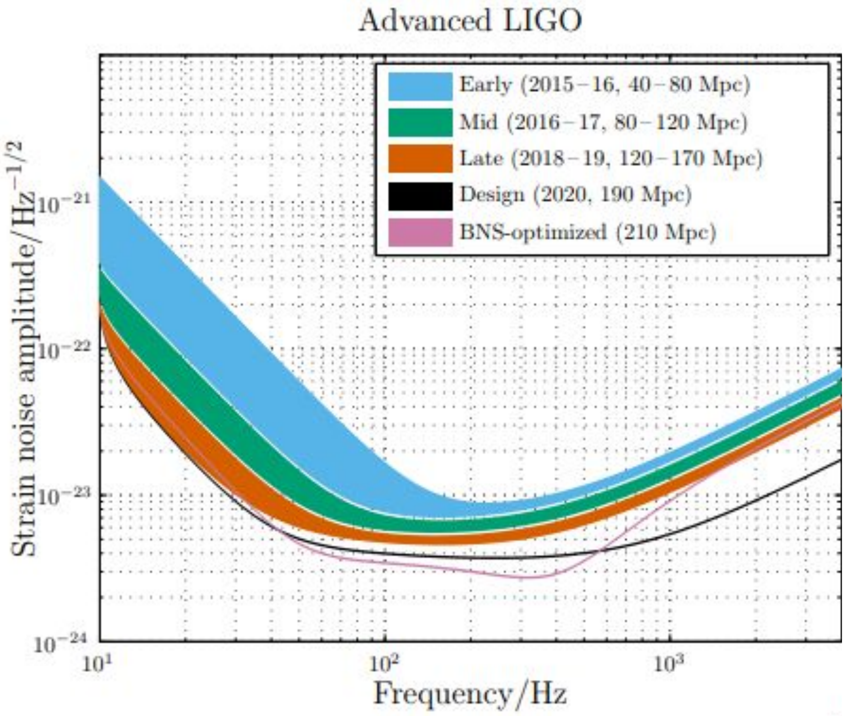

circa GW170817

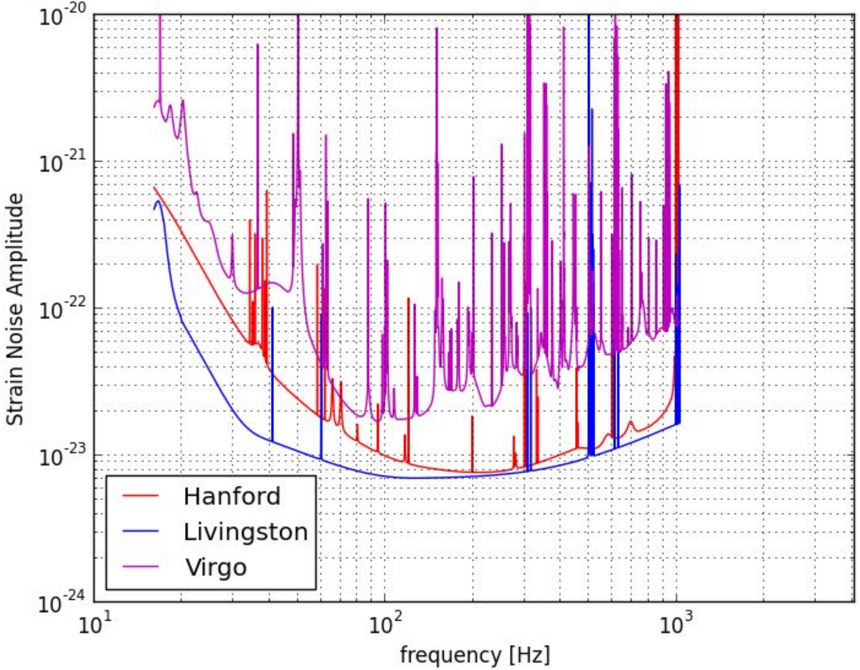

Abbott+(2018)

Our detectors

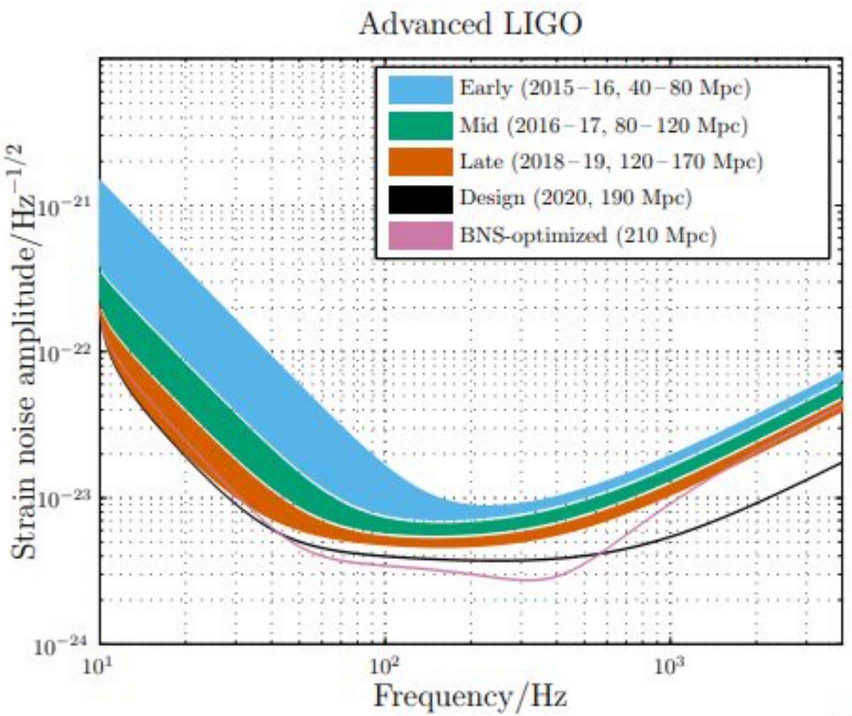

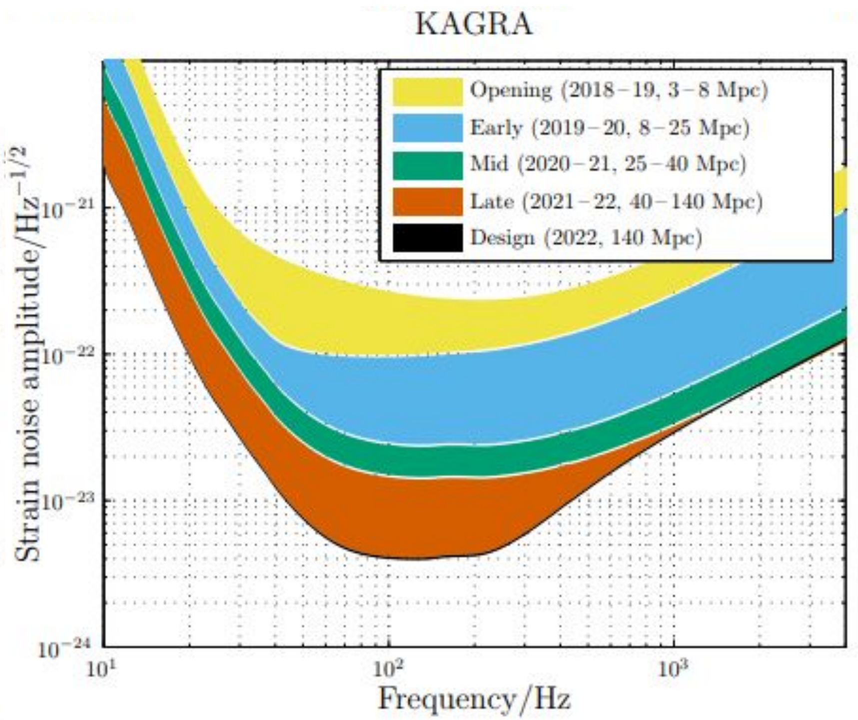

Abbott+(2018)

Types of signals that *have* been observed

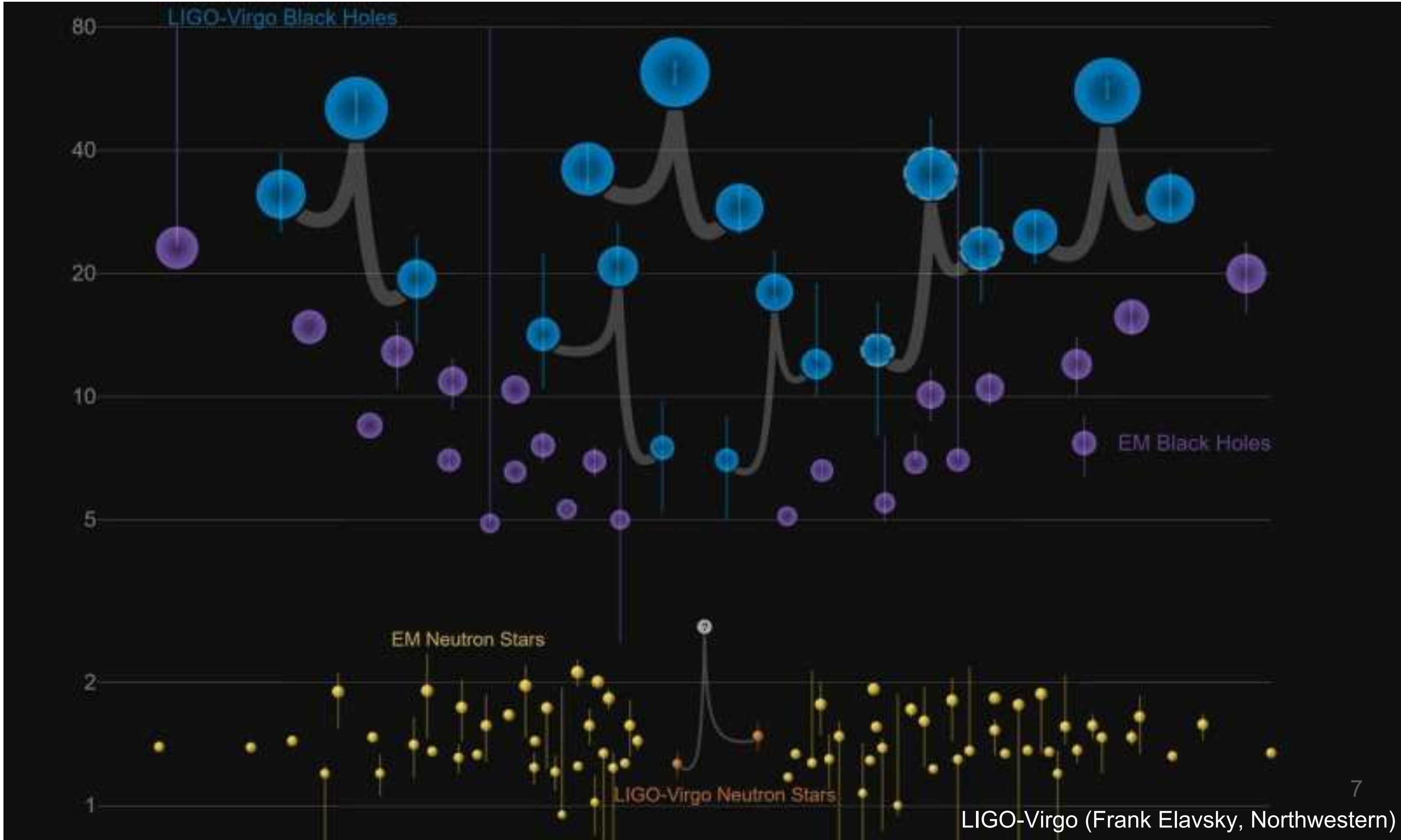

LIGO-Virgo (Frank Elavsky, Northwestern)

Types of signals that *have* been observed

$$p\left(m_1,m_2 \mid \alpha,M_{\max}\right) \propto \frac{m_1^{-\alpha}\,\mathcal{H}(M_{\max}-m_1)}{\min(m_1,M_{\mathrm{tot,max}}-m_1)-M_{\min}}$$

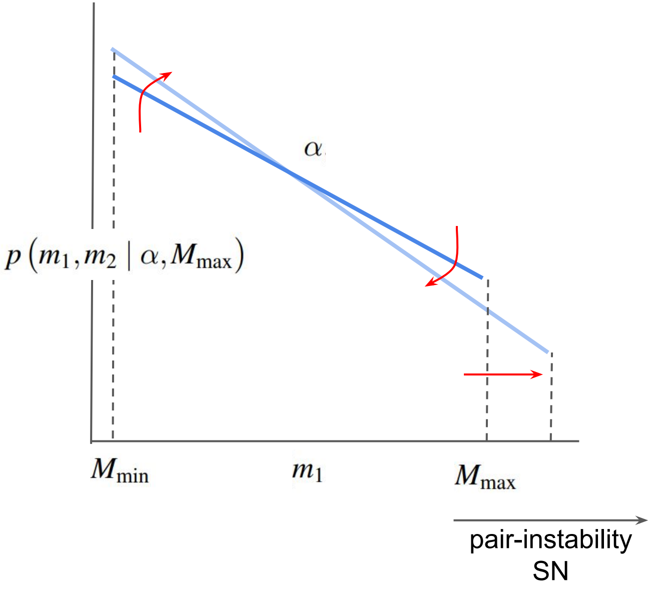

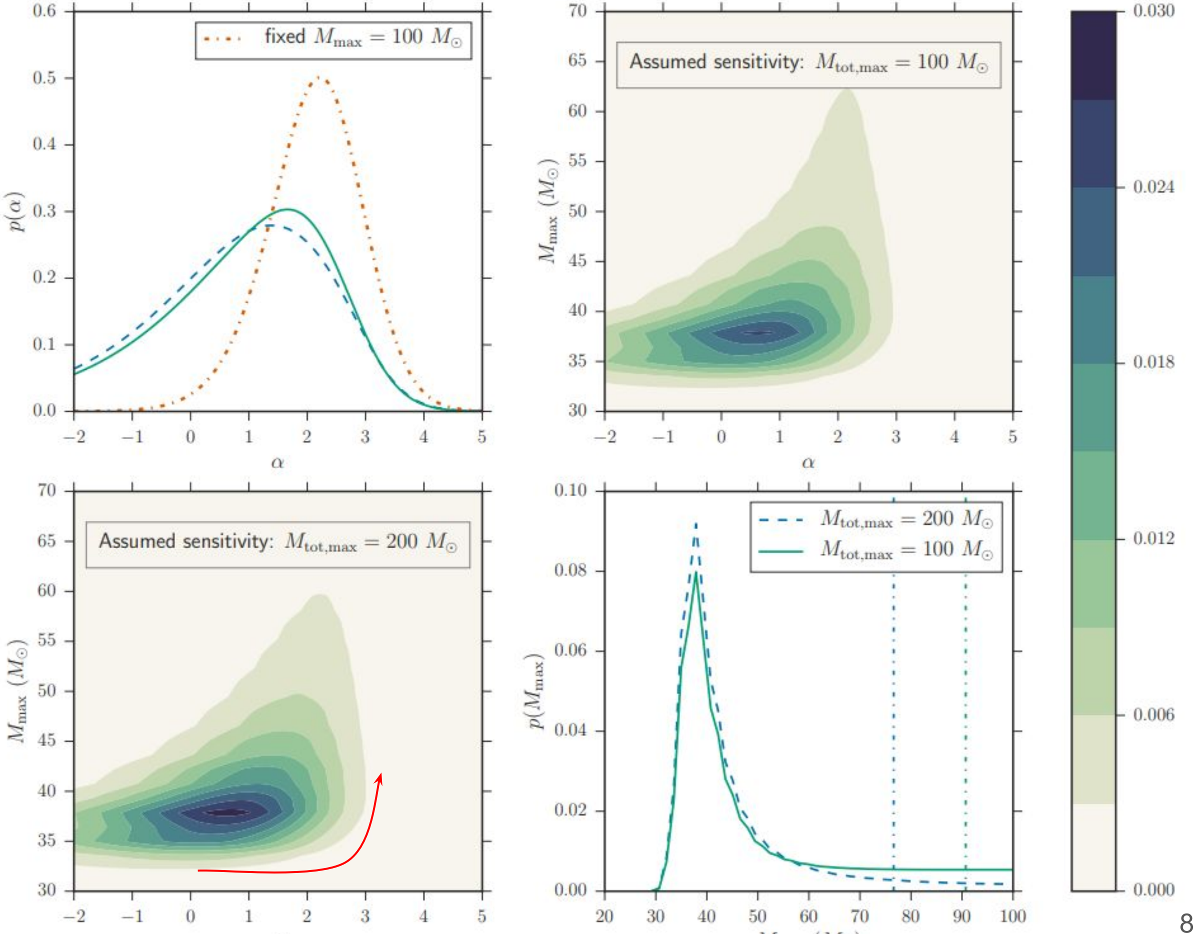

arXiv:1709.08584

Types of signals that *have* been observed

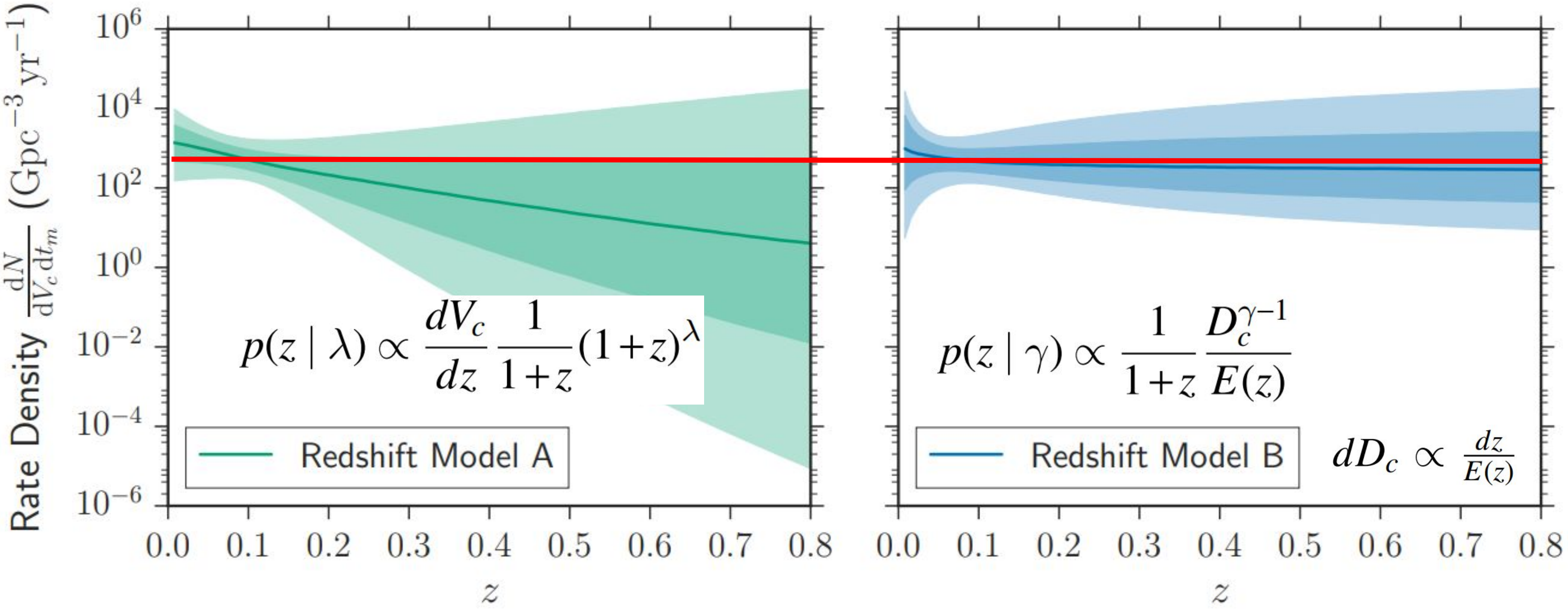

2 ~ad hoc models, both are consistent with a constant merger rate as a function of redshift.

arXiv:1805.10270

Science enabled by observed signals

Tests of General Relativity

speed of gravity/mass of graviton: ApJL 848, 2 (2017)

implications for early-universe cosmology: PRD 97, 084005 (2018)

deviations from post-newtonian waveform: PRL 116, 221101 (2016)

scalar, vector vs. tensor polarizations: PRL 119, 141104 (2017)

limits on the number of spacetime dimensions from GW170817: arXiv:1801.08160 (2018)

and many more!

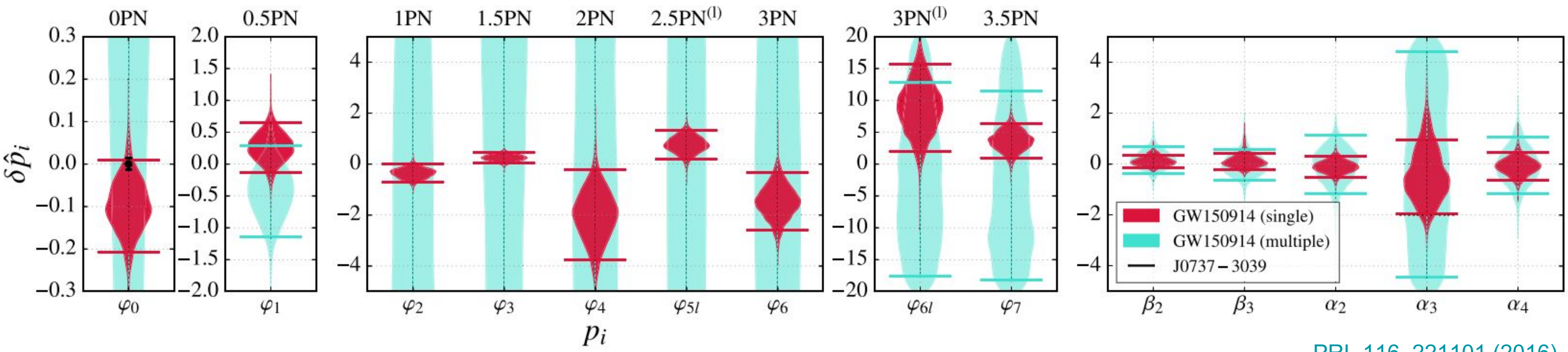

PRL 116, 221101 (2016)

Science enabled by observed signals

stellar and galactic physics

GW150914 (see ApJL 818, 2 (2016))

Big black holes exist and merge!
- → Relatively weak stellar winds (at low metallicities)
- → SN kicks must be relatively small to keep system bound

Possible formation channels
- → isolated evolution
- → dynamical interactions within Globular Clusters

These could be distinguished by the component spins and their alignment with the orbital angular momentum or by the precise merger rate as a function of redshift.

GW170817 (see ApJL 850, 2 (2017))

As long as merger delay times are ≳ 1 Gyr, constraints do not strongly depend on Galaxy profile, Star Formation Rate, etc
- → at a projected distance of ~ 2kpc, dynamical timescales within the galaxy are ~20 Myr
- → SN kicks must be relatively small to keep system bound

"An increased source sample resulting from future GW data will of course better constrain the merger rates, but will also allow us to probe the mass distributions and any dependence on redshift. To go beyond the current, mostly qualitative discussion, and move toward comprehensive model constraints, ***it will be important to develop frameworks that account for observational biases and for appropriate sampling of the model parameter space including relevant parameter degeneracies***."

Science enabled by observed signals

Neutron Star Equation of State measurements

Tides!: arXiv:1805.11579 (2018)
Equation of State inference: arXiv:1805.11581 (2018)

R(m, stiff)
Λ(m, stiff)

R(m, soft)
Λ(m, soft)

stiff → large radii

soft → small radii

For the same mass, soft EOS “collapse more” under their own weight.

Science enabled by observed signals

Neutron Star Equation of State measurements

Tides!: arXiv:1805.11579 (2018)
Equation of State inference: arXiv:1805.11581 (2018)

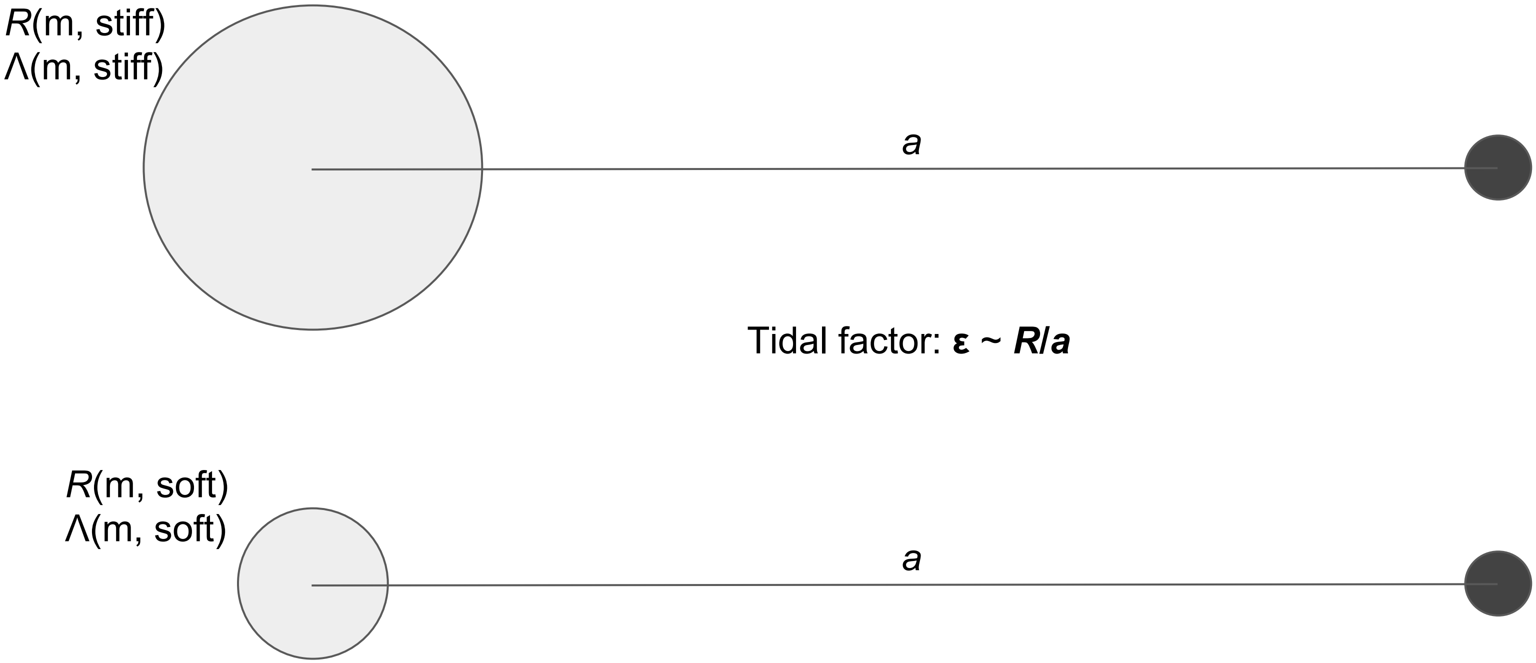

Tidal factor: **$\varepsilon \sim R/a$**

Science enabled by observed signals

Neutron Star Equation of State measurements

Tides!: [arXiv:1805.11579 (2018)](arXiv:1805.11579)
Equation of State inference: [arXiv:1805.11581 (2018)](arXiv:1805.11581)

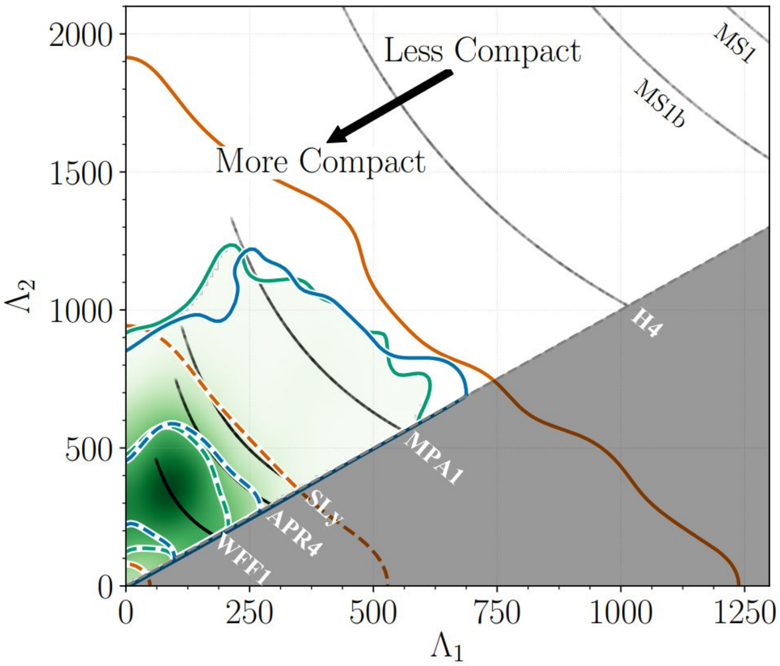

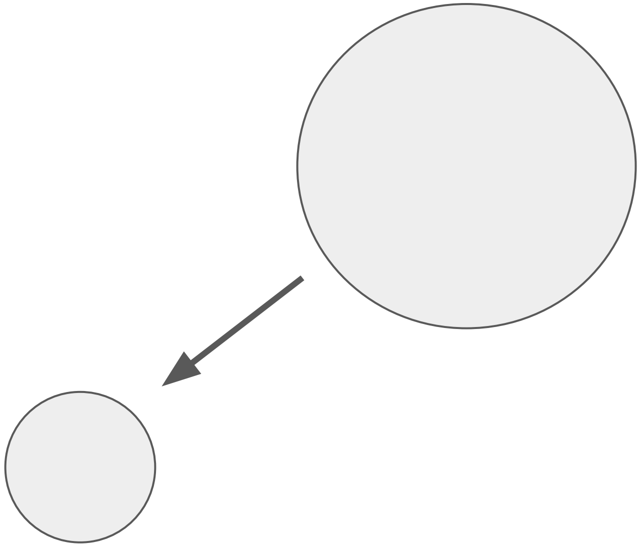

Less Compact

More Compact

Science enabled by observed signals

Neutron Star Equation of State measurements

Tides!: arXiv:1805.11579 (2018)
Equation of State inference: arXiv:1805.11581 (2018)

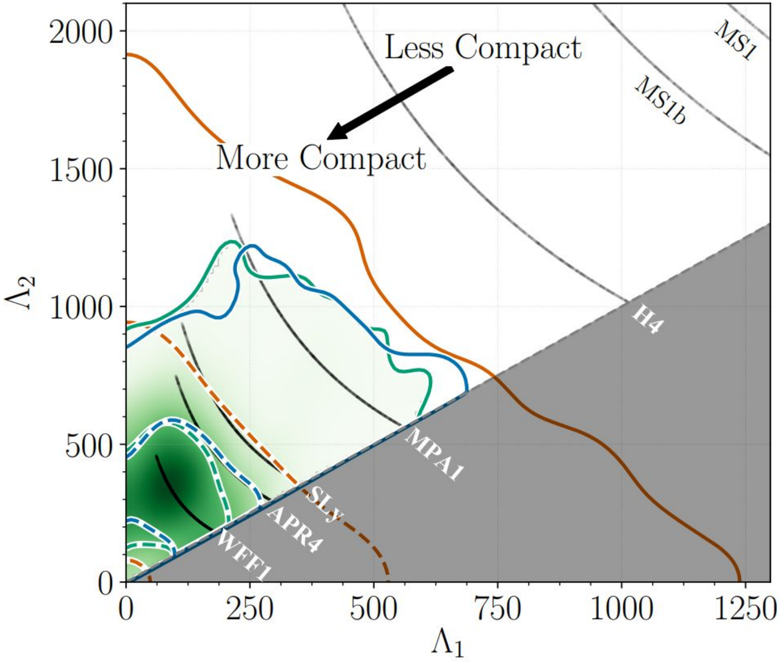

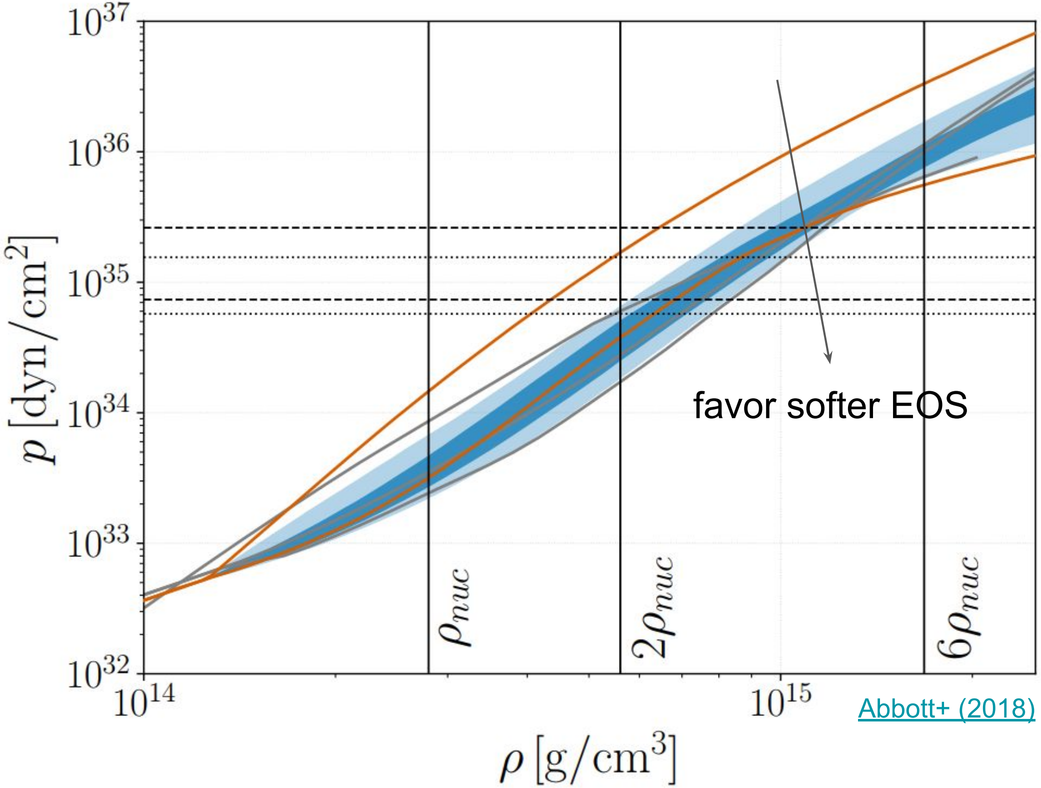

favor softer EOS

Abbott+ (2018)

Science enabled by observed signals

Neutron Star Equation of State measurements

Tides!: [arXiv:1805.11579 (2018)](https://arxiv.org/abs/1805.11579)
Equation of State inference: [arXiv:1805.11581 (2018)](https://arxiv.org/abs/1805.11581)

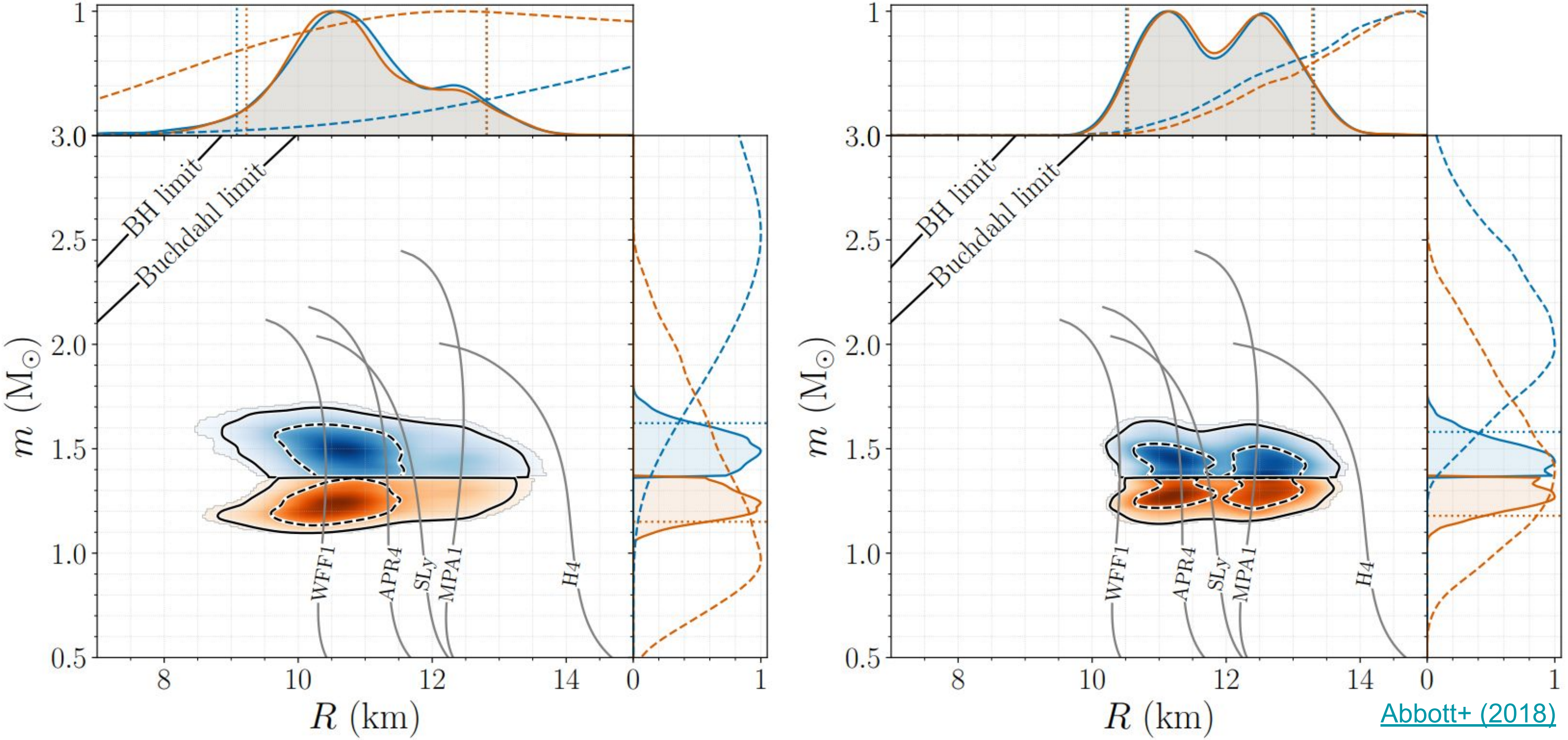

[Abbott+ (2018)](https://arxiv.org/abs/1805.11581)

Science enabled by observed signals

Nonlinear Tidal instabilities

modes' dynamics described in a spherical harmonic Galerkin decomposition

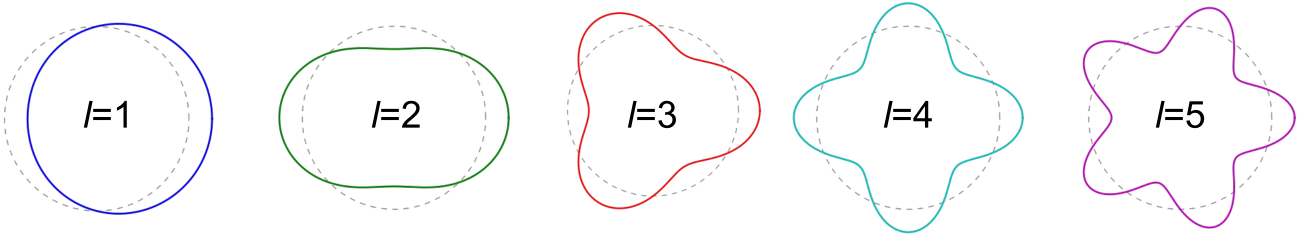

Tides excite stellar normal modes, which evolve independently in linear theory.

Nonlinear interactions couple (many) different modes together with associated coupling coefficients and instability thresholds.

The ***p-g* instability** couples the linear tidal bulge to a ***high-frequency p-mode*** and a ***low-frequency g-mode***. This instability ***grows secularly*** throughout the orbit once tripped.

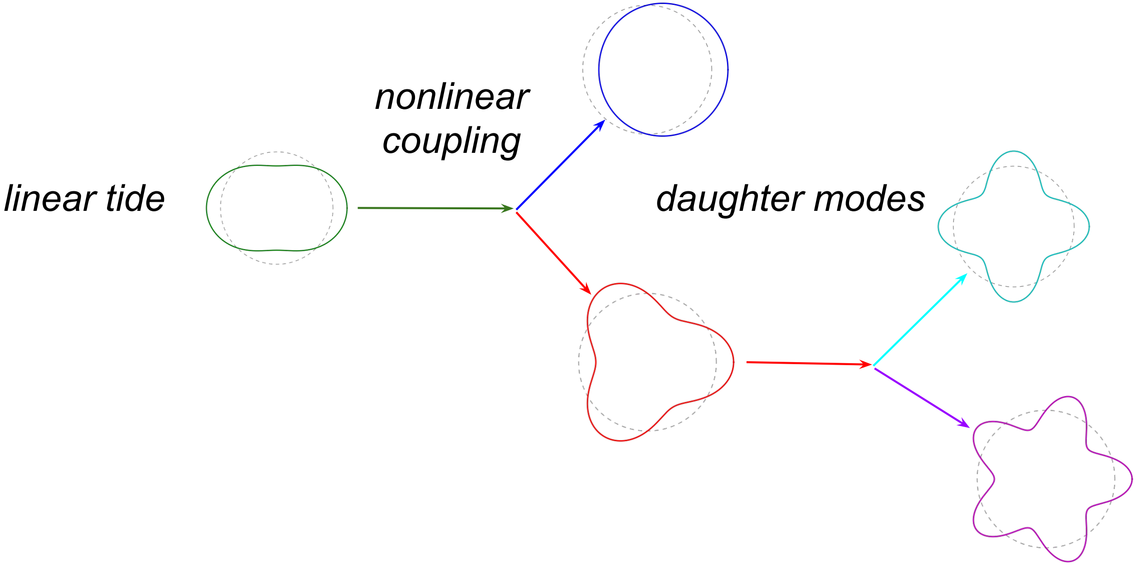

Science enabled by observed signals

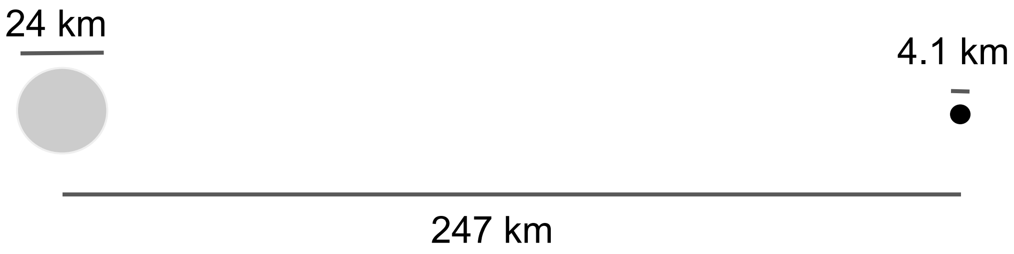

Nonlinear Tidal instabilities

p-g secular tidal instability could introduce phase shifts into the observed waveform by providing an additional energy loss mechanism.

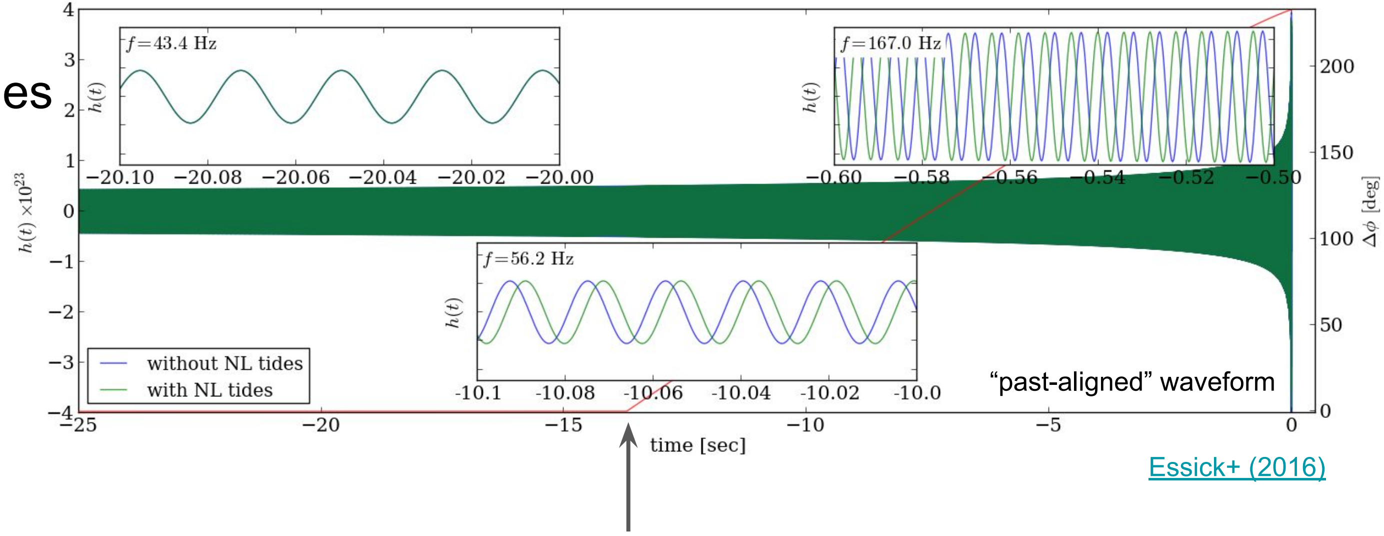

"past-aligned" waveform

Essick+ (2016)

p-g instability turns on at $f_{GW} \sim 50$ Hz

Science enabled by observed signals

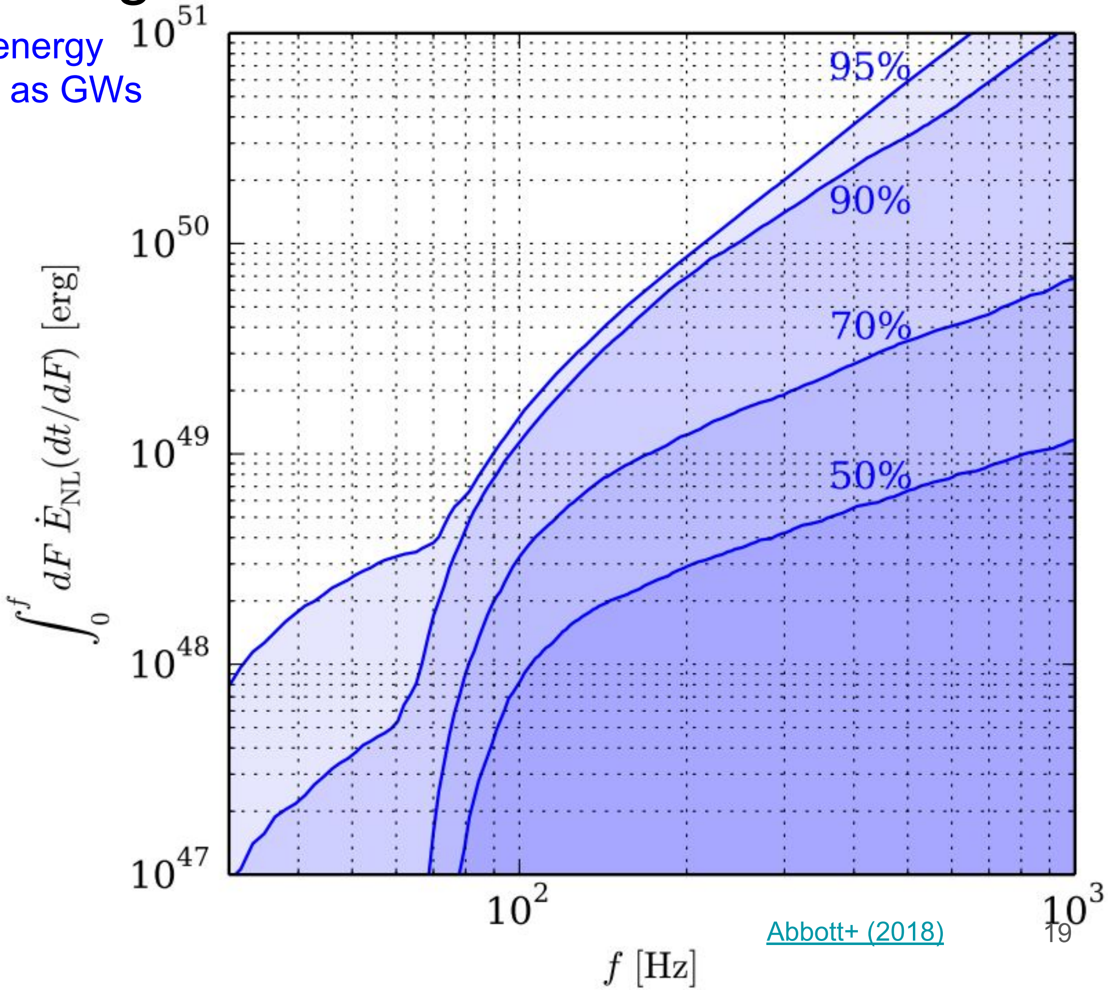

Abbott+ (2018)

Nonlinear Tidal instabilities

p-g secular tidal instability could introduce phase shifts into the observed waveform by providing an additional energy loss mechanism.

What I’m personally excited about for O3

new signals and ***more*** signals

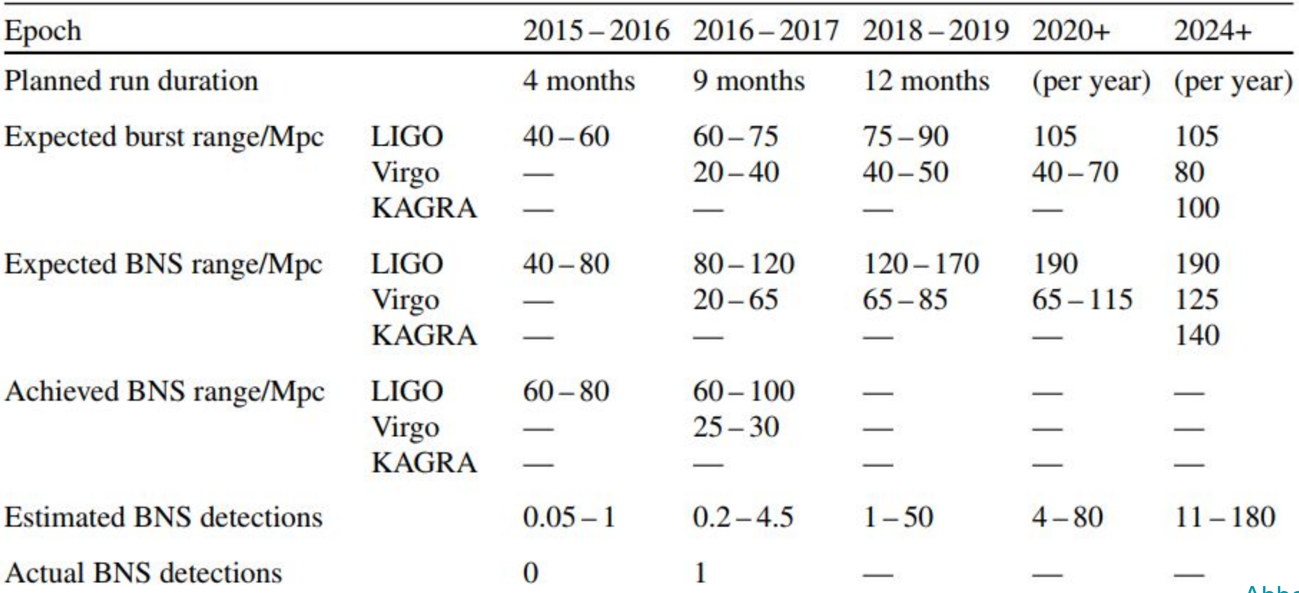

Epoch		2015 – 2016	2016 – 2017	2018 – 2019	2020+	2024+
Planned run duration		4 months	9 months	12 months	(per year)	(per year)
Expected burst range/Mpc	LIGO	40 – 60	60 – 75	75 – 90	105	105
	Virgo	—	20 – 40	40 – 50	40 – 70	80
	KAGRA	—	—	—	—	100
Expected BNS range/Mpc	LIGO	40 – 80	80 – 120	120 – 170	190	190
	Virgo	—	20 – 65	65 – 85	65 – 115	125
	KAGRA	—	—	—	—	140
Achieved BNS range/Mpc	LIGO	60 – 80	60 – 100	—	—	—
	Virgo	—	25 – 30	—	—	—
	KAGRA	—	—	—	—	—
Estimated BNS detections		0.05 – 1	0.2 – 4.5	1 – 50	4 – 80	11 – 180
Actual BNS detections		0	1	—	—	—

Abbott+(2018)

What I’m personally excited about for O3

data quality automation

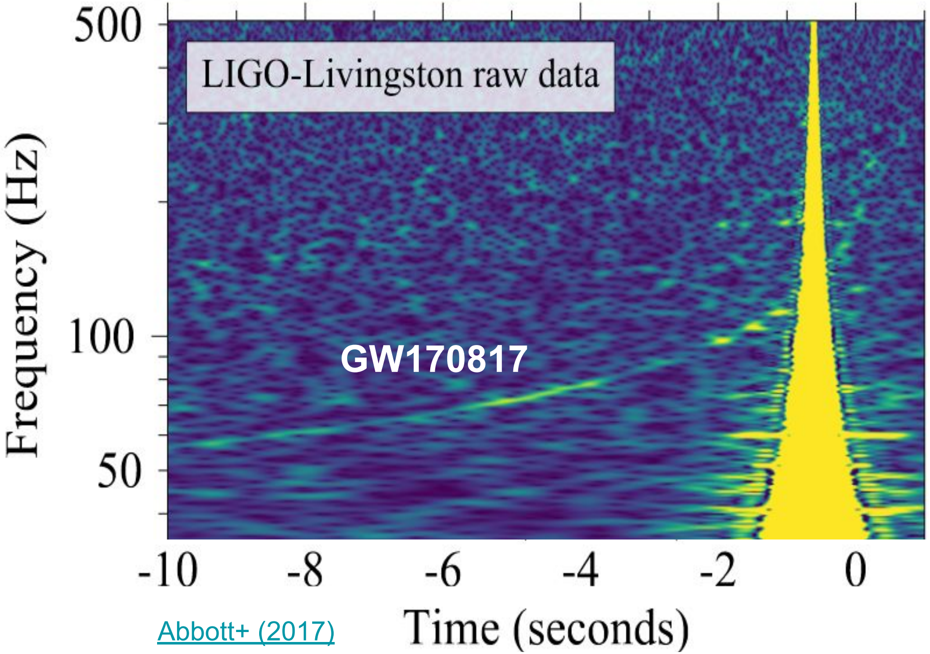

Abbott+ (2017)

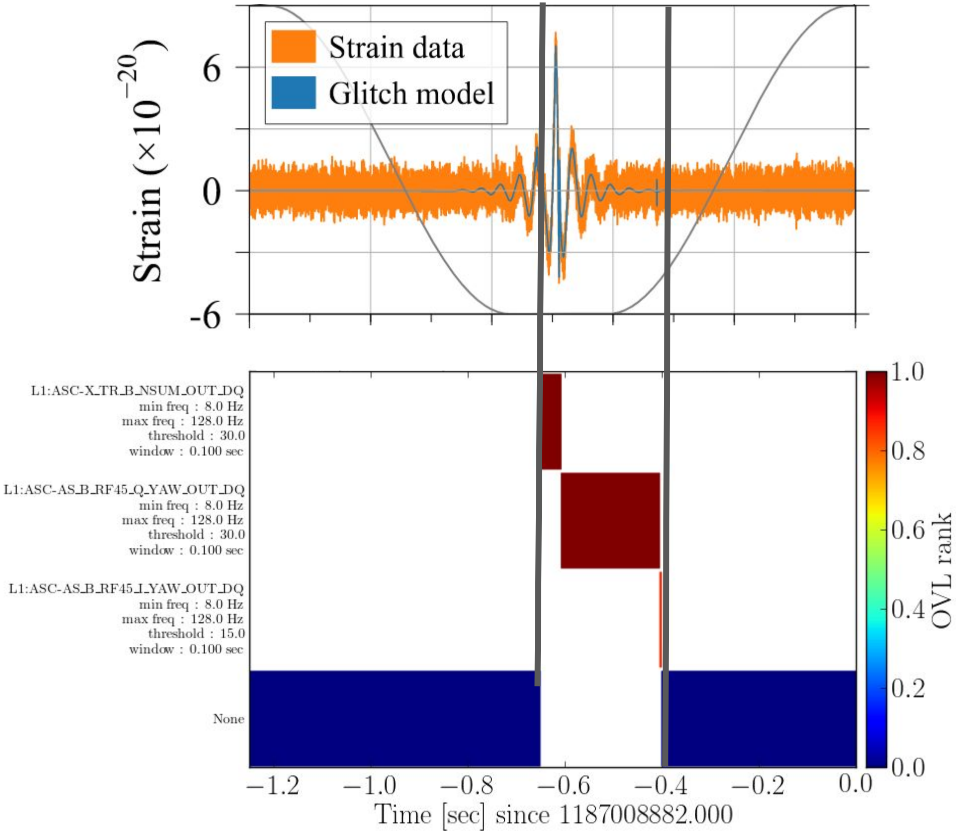

automatically available within **9 sec**

References

GW170817: Observation of Gravitational Waves from a Binary Neutron Star Inspiral. PRL 119, 161101 (2017).
Prospects for observing and localizing gravitational-wave transients with Advanced LIGO, Advanced Virgo and KAGRA. Living Reviews in Relativity (2018)
Limits on the number of spacetime dimensions from GW170817. arXiv:1801.08160
Astrophysical Implications of the binary black hole merger GW150914. ApJL 818, 2 (2016).
Speed of gravitational waves and black hole hair. PRD 97, 084005 (2018).
GW170817: Measurements of neutron star radii and equation of state. arXiv:1805.11581 (2018).
Properties of the binary neutron star merger GW170817. arXiv:1805.11579 (2018).
GW170814: A three-detector observation of gravitational waves from a binary black hole coalescence. PRL 119, 141101 (2017).
Tests of General Relativity with GW150914. PRL 116, 221101 (2016).
Gravitational waves and gamma-rays from a binary neutron star merger: GW170817 and GRB170817A. ApJL 848, 2 (2017).
Estimating the contribution of dynamical ejecta in the kilonova associated with GW170817. ApJL 850, 2 (2017).
On the progenitor of binary neutron star merger GW170817. ApJL 850, 2 (2017).
How many kilonovae can be found in past, present, and future survey data sets? ApJL 852, 1 (2017).
A gravitational-wave standard siren measurement of the Hubble constant. Nature 551, 85-88 (2017).
Precision standard siren cosmology. arXiv:1712.06531 (2017).
Where are LIGO's big black holes? ApJL 851, 2 (2017).
Does the black hole merger rate evolve with redshift? arXiv:1805.10270 (2018).
Observational selection effects with ground-based gravitational wave detectors. ApJ 835, 1 (2017).
Impact of the tidal $p - g$ instability on the gravitational wave signal from coalescing binary neutron stars. PRD 94, 103012 (2016).
Constraining the p-mode -- g-mode tidal instability with GW170817. arXiv:1808.08676.

Detection Methods

unmodeled searches

Detection Methods

matched filter

Science enabled by observed signals

Nonlinear Tidal instabilities

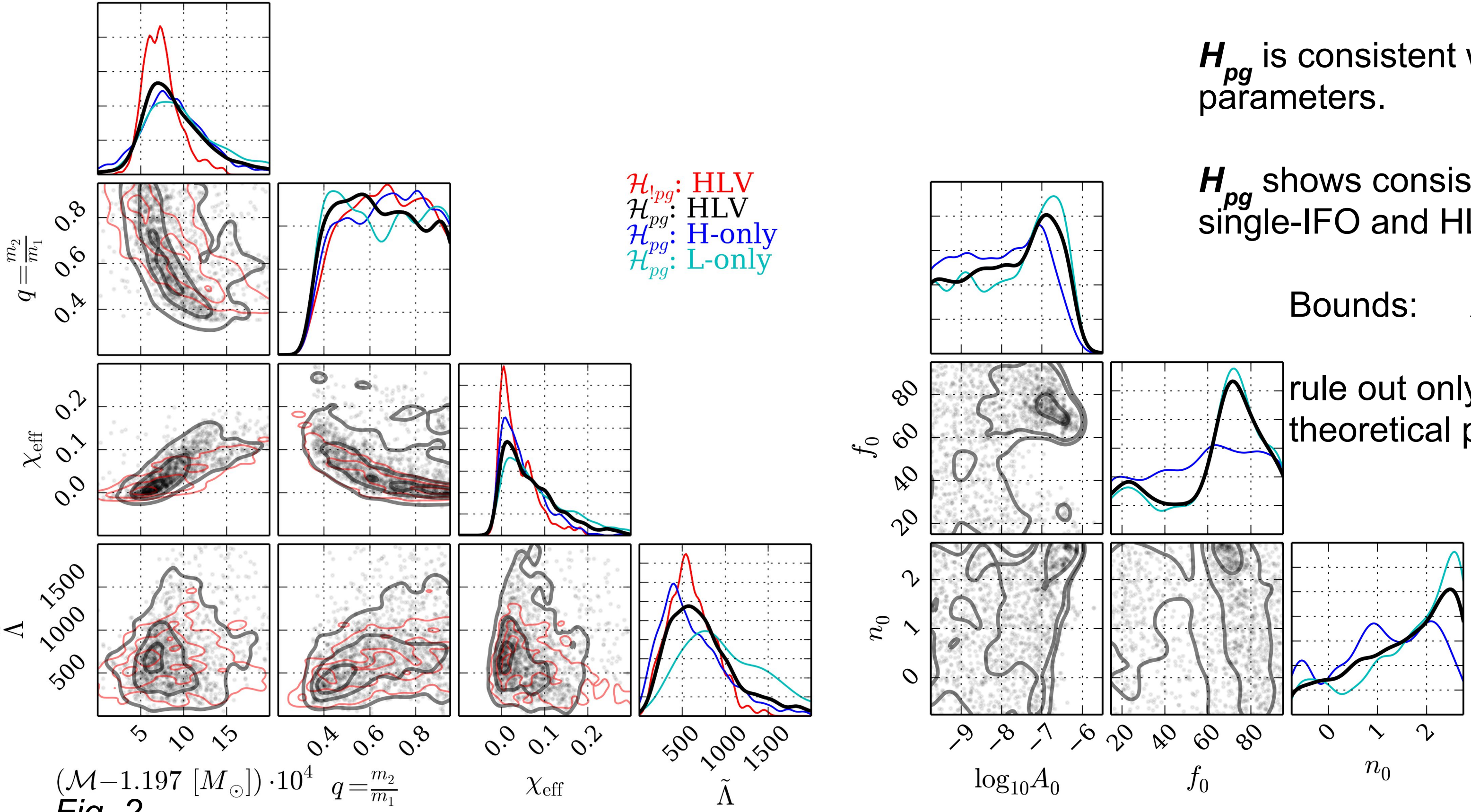

Fig. 2

H $_{pg}$ is consistent with ***H*** $_{!pg}$ for shared parameters.

H $_{pg}$ shows consistent behavior with single-IFO and HLV data.

Bounds: $\boldsymbol{A_0 \leq 3.3\times10^{-7}}$
$\boldsymbol{f_0 \sim 70}$ **Hz**
rule out only the most extreme theoretical predictions (A_0~10^{-6})

Challenges

- ~200,000 channels per site
    - **~6,000** “fast” channels
- Glitch rates ~1/100 sec
    - ***Non-stationary!***

- post facto
    - latency < **60 sec**
- pre-filtering
    - latency < **1 sec**

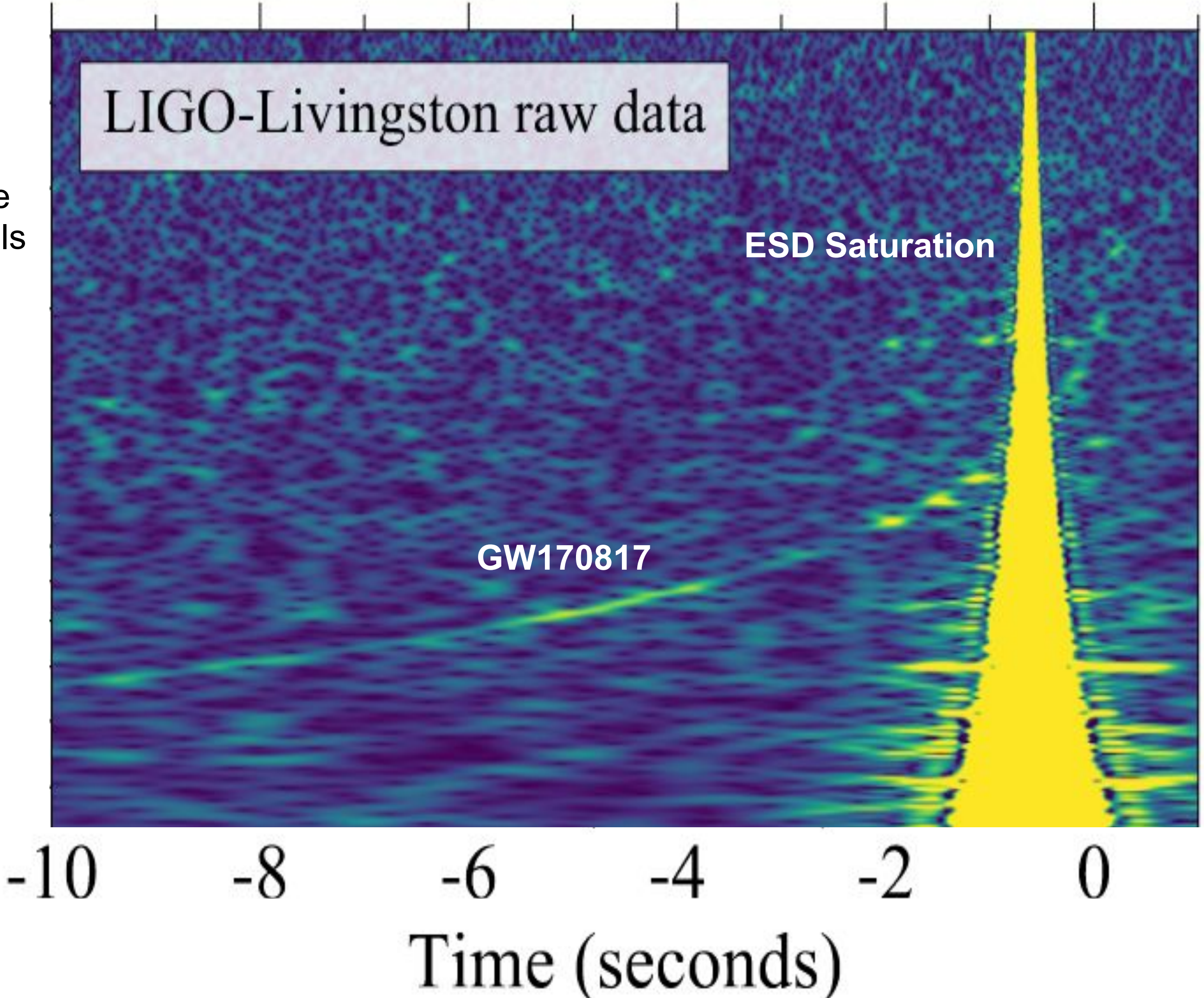

Challenges

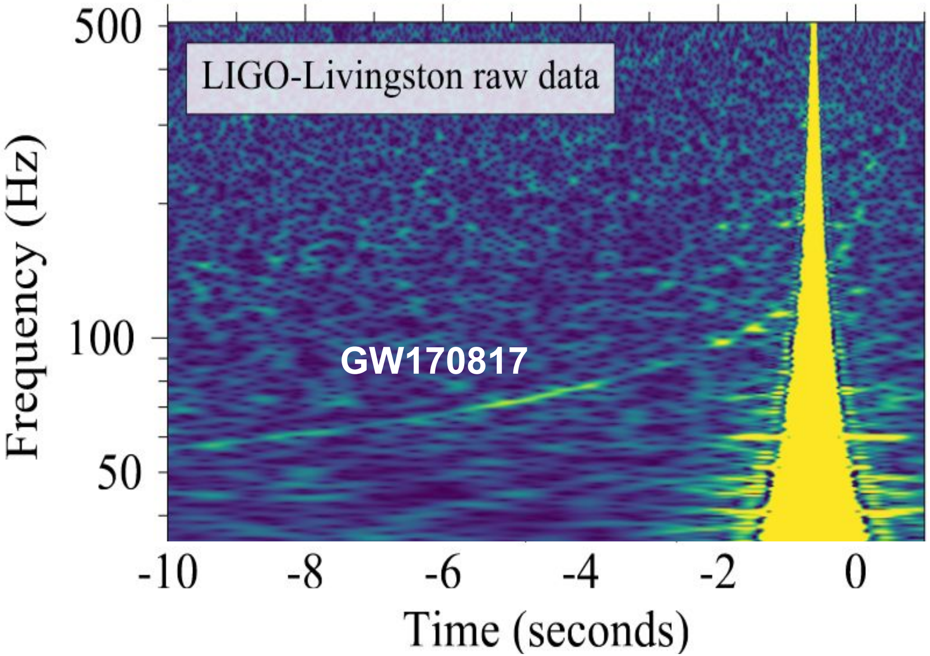

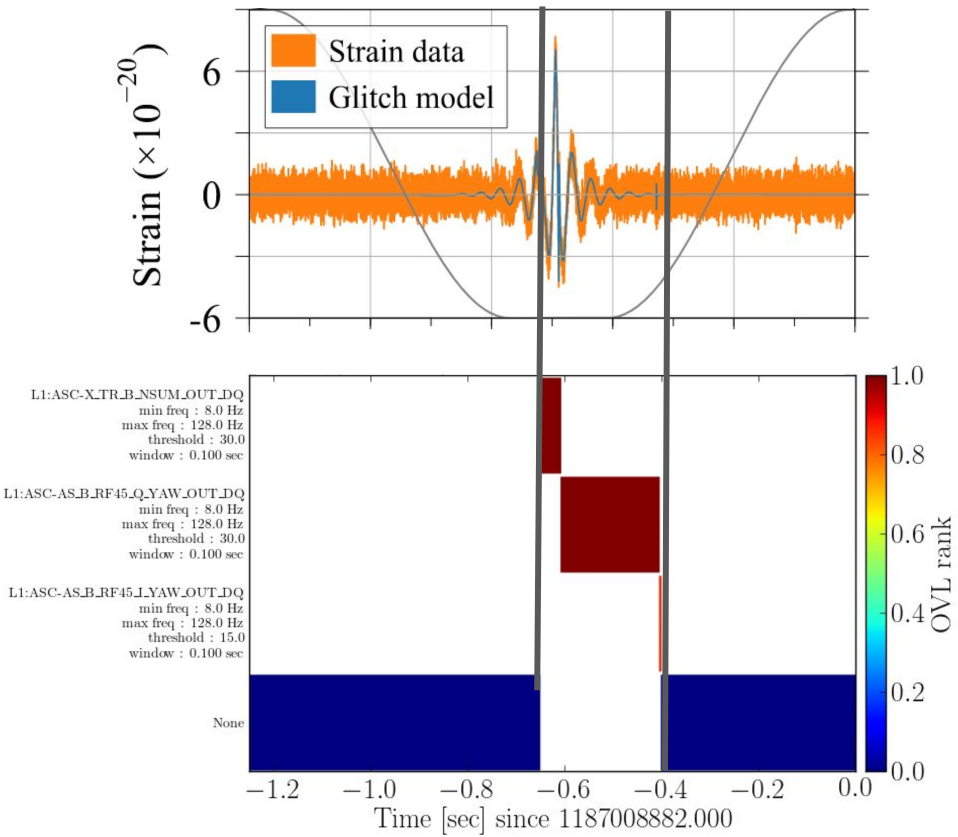

automatically available within **9 sec**

Challenges

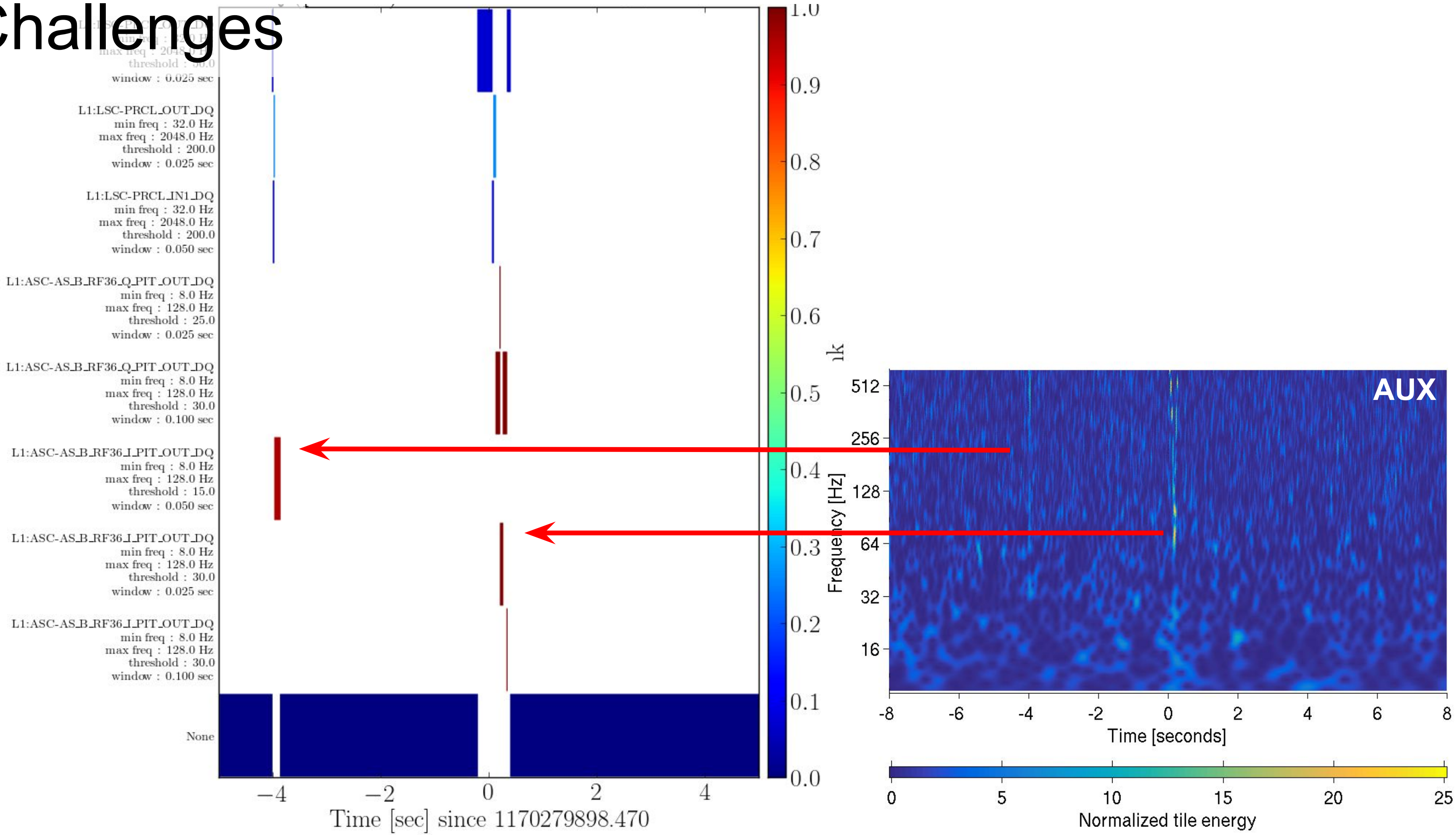
L1:LSC-PRCL_OUT_DQ
min freq : 32.0 Hz
max freq : 2048.0 Hz
threshold : 50.0
window : 0.025 sec
L1:LSC-PRCL_OUT_DQ
min freq : 32.0 Hz
max freq : 2048.0 Hz
threshold : 200.0
window : 0.025 sec
L1:LSC-PRCL_IN1_DQ
min freq : 32.0 Hz
max freq : 2048.0 Hz
threshold : 200.0
window : 0.050 sec
L1:ASC-AS_B_RF36_Q_PIT_OUT_DQ
min freq : 8.0 Hz
max freq : 128.0 Hz
threshold : 25.0
window : 0.025 sec
L1:ASC-AS_B_RF36_Q_PIT_OUT_DQ
min freq : 8.0 Hz
max freq : 128.0 Hz
threshold : 30.0
window : 0.100 sec
L1:ASC-AS_B_RF36_I_PIT_OUT_DQ
min freq : 8.0 Hz
max freq : 128.0 Hz
threshold : 15.0
window : 0.050 sec
L1:ASC-AS_B_RF36_I_PIT_OUT_DQ
min freq : 8.0 Hz
max freq : 128.0 Hz
threshold : 30.0
window : 0.025 sec
L1:ASC-AS_B_RF36_I_PIT_OUT_DQ
min freq : 8.0 Hz
max freq : 128.0 Hz
threshold : 30.0
window : 0.100 sec
None
−4
−2
0
2
4
Time [sec] since 1170279898.470
1.0
0.9
0.8
0.7
0.6
0.5
0.4
0.3
0.2
0.1
0.0
AUX
512
256
128
64
32
16
Frequency [Hz]
-8
-6
-4
-2
0
2
4
6
8
Time [seconds]
0
5
10
15
20
25
Normalized tile energy

Challenges

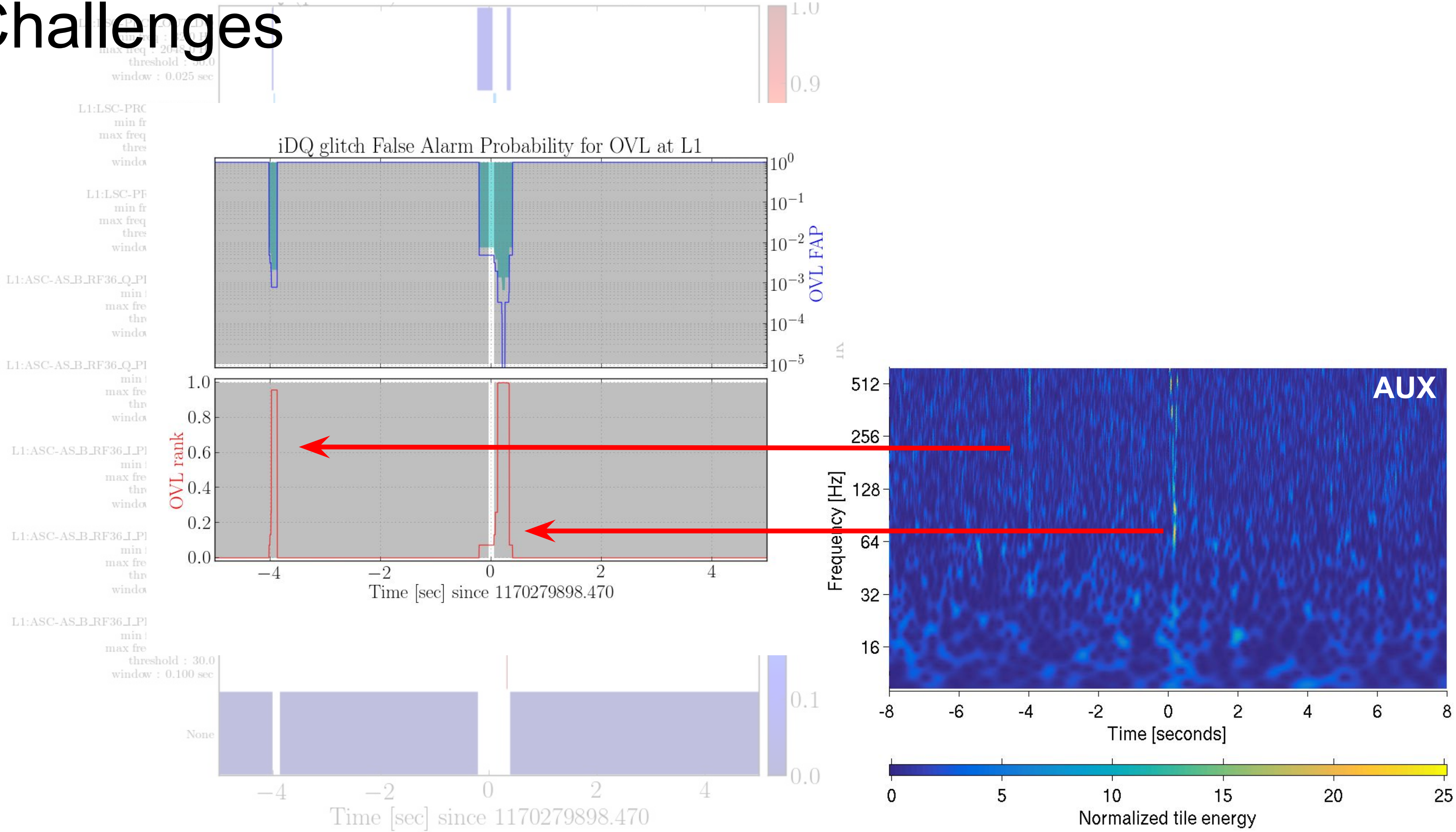
iDQ glitch False Alarm Probability for OVL at L1
10^{0}
10^{-1}
10^{-2}
10^{-3}
10^{-4}
10^{-5}
OVL FAP
1.0
0.8
0.6
0.4
0.2
0.0
OVL rank
−4
−2
0
2
4
Time [sec] since 1170279898.470
L1:LSC-PRC
L1:LSC-PR
L1:ASC-AS_B_RF36_Q_PI
L1:ASC-AS_B_RF36_I_PI
min fr
max freq
threshold : 30.0
window : 0.025 sec
window : 0.100 sec
None
1.0
0.9
0.1
0.0
AUX
512
256
128
64
32
16
Frequency [Hz]
-8
-6
-4
-2
0
2
4
6
8
Time [seconds]
0
5
10
15
20
25
Normalized tile energy

Challenges

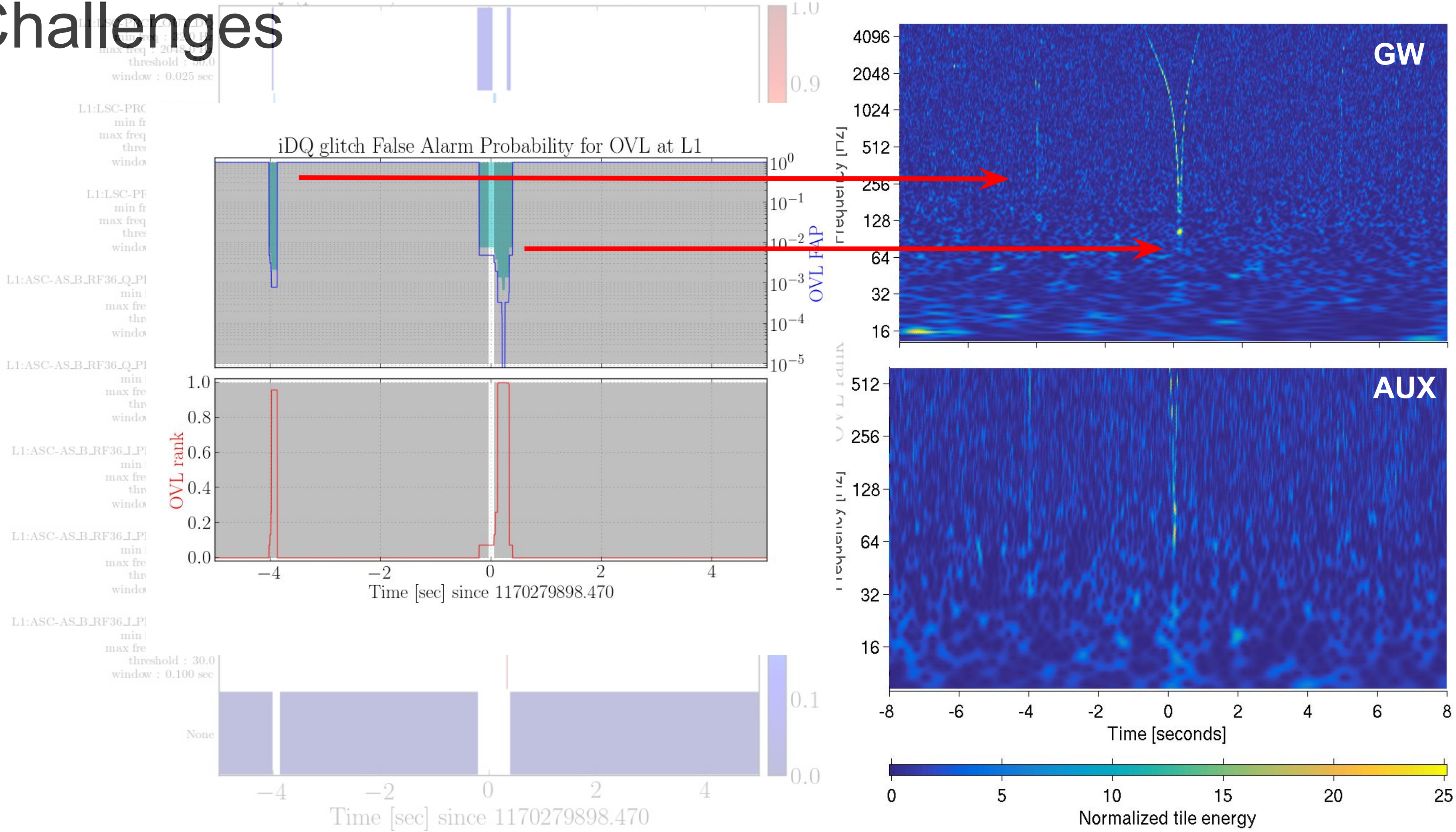
iDQ glitch False Alarm Probability for OVL at L1
OVL FAP
10^0
10^{-1}
10^{-2}
10^{-3}
10^{-4}
10^{-5}
OVL rank
1.0
0.8
0.6
0.4
0.2
0.0
−4
−2
0
2
4
Time [sec] since 1170279898.470
L1:LSC-PRC
L1:ASC-AS_B_RF36_Q_PI
L1:ASC-AS_B_RF36_I_PI
threshold : 30.0
window : 0.025 sec
window : 0.100 sec
None
GW
AUX
4096
2048
1024
512
256
128
64
32
16
-8
-6
-4
-2
0
2
4
6
8
Time [seconds]
0
5
10
15
20
25
Normalized tile energy